ELSEVIER

International Journal of Mass Spectrometry 179/180 (1998) 91–102

Studying protonated ion hydration by infrared spectroscopy of size-selected $NH_4^+(H_2O)_n$ clusters in a free jet expansion

Hai-Chou Chang[a], Yih-Sheng Wang[b], Yuan T. Lee[a,b], and Huan-Cheng Chang[a,]*

[a]Institute of Atomic and Molecular Sciences, Academia Sinica, P.O. Box 23-166, Taipei, Taiwan 106, Republic of China
[b]Department of Chemistry, National Taiwan University, Taipei, Taiwan 106, Republic of China

Received 23 March 1998; accepted 1 June 1998

Abstract

This paper investigates heterogeneous water nucleation on ammonium ions in a supersonic jet using vibrational predissociation spectroscopy. For $NH_4^+(H_2O)_n$, it is revealed that nonhydrogen bonded NH stretching of NH_4^+ is resonant at 3300–3400 cm^{-1}, which is fairly independent of the cluster size of $n = 2–4$. The frequencies, however, shift strongly from ~2900 cm^{-1} of $n = 2$ to ~3100 cm^{-1} of $n = 4$ for hydrogen bonded NH stretches. Hydration at the second shell starting with $n = 5$ has little effect on the ion core vibrations. Similar to the NH oscillations, nonhydrogen bonded and hydrogen bonded OH stretches are found for the solvent molecules at 3600–3800 and 3300–3600 cm^{-1}, respectively. Simultaneous observations of these four distinct stretches allow us to identify a number of structural isomers (both cyclic and noncyclic) at $n = 4–6$. Of particular interest is that the clusters form an energetically favored four-membered ring at $n = 5$ that is evidenced by its characteristic bonded OH stretching absorptions at ~3550 cm^{-1}. This ring shaped structure remains at $n \geq 5$, where a sharp feature that can be ascribed to the nonhydrogen bonded OH stretching of three-coordinated H_2O emerges at ~3690 cm^{-1}. All the results, both frequencies and assignments, are in close agreement with recent ab initio calculations. The association of the present observations with heterogeneous water nucleation in the gas phase and the infrared spectroscopy of neutral water clusters and crystalline ice is discussed. (Int J Mass Spectrom 179/180 (1998) 91–102) © 1998 Elsevier Science B.V.

Keywords: Ion association; Hydrated ammonium ion; Jet-cooled isomeric clusters; Hydrogen bond; Vibrational predissociation spectroscopy

1. Introduction

Protonated ions are ubiquitous in aqueous solutions. They play important roles in many organic and biological reactions as reactants, intermediates, and products. Particularly for amines, they can be easily protonated because of intrinsic basicity [1]. The protonated amines have frequently been used as model molecules to study the structure and function of biomolecules since they are prototypes of amino groups in peptides and proteins [2]. Among all amines, the simplest is NH_3. In acidic solutions, NH_3 is protonated to yield NH_4^+, which forms strong hydrogen bonds with water. Over the past few decades, the studies on amine hydration have been limited to solution phases employing nuclear magnetic resonance (NMR) spectroscopy [3]. However,

---

* Corresponding author.

Dedicated to Professor Fulvio Cacace in recognition of his outstanding contributions for many decades to gas-phase ion chemistry and physics.

PII S1387-3806(98)14065-4

Table 1
Hydration energies of the clustering reaction, $NH_4^+S_{n-1} + S \rightarrow NH_4^+S_n$, where S = NH_3 and H_2O

	$\Delta H^\circ_{n-1,n}$ (kcal mol^{-1})				
	S = H_2O		S = NH_3		
$n-1, n$	PCK[a]	M[b]	SK[c]	PCK[a]	AF[d]
0, 1	−17.3	−19.9	−27	−24.8	−21.5
1, 2	−14.7	−12.4	−17	−17.5	−16.2
2, 3	−13.4	−12.2	−16.5	−13.8	−13.5
3, 4	−12.2	−10.8	−14.5	−12.5	−11.7
4, 5	−9.7	−10.6	−7.5	−9.5	−7.0
5, 6		−9.1			−6.5
6, 7		−8.4			

[a] J.D. Payzant, A.J. Cunningham, P. Kebarle, Can. J. Chem. 51 (1973) 3252.
[b] [8].
[c] S.K. Searles, P. Kebarle, J. Phys. Chem. 72 (1968) 742.
[d] M.R. Arshadi, J.H. Futrell, J. Phys. Chem. 78 (1974) 1482.

due to complications arising from many-body intermolecular interactions and rapid proton exchange between solutes and solvents, the results have often been inconclusive. Studying ion hydration in the gas phase offers an alternative approach, but experiments of this type have rarely been reported, largely because of the difficulty of generating sufficient amounts of ions for investigation. A noticeable exception is pulsed electron high pressure mass spectrometry, which has been used to successfully determine the heat of formation and hydration in a variety of protonated amine clusters. Kebarle [4] provided a critical review on this subject; however, as conveyed by that article, nearly all the prevailing results are limited to thermochemistry and kinetics measurements. Detailed spectroscopic investigation [5] of ammonium ion hydration in the gas phase is still lacking.

There have been a number of theoretical [6,7] and experimental studies [8] for small $NH_4^+(H_2O)_n$ ions regarding the heat of hydration $\Delta H^\circ_{n-1,n}$ of

$$NH_4^+(H_2O)_{n-1} + H_2O \rightarrow NH_4^+(H_2O)_n \qquad (1)$$

The energy released when the first hydrogen bond is formed is $-\Delta H^\circ_{0,1} \sim 19$ kcal mol^{-1}, which decreases monotonically with an increasing n to ~9 kcal mol^{-1} at $n > 5$ (Table 1). Calculations for clusters at potential minima indicate that the first hydration shell contains four H_2O molecules, symmetrically linked to the central ion with four hydrogen bonds. Inserting the fifth H_2O into the first shell is energetically unfavored by about 5 kcal mol^{-1} [7], as compared to positioning it on the second shell. Along with the energetics calculations, rotational dynamics simulations [9,10] have also been performed. The simulations were primarily motivated by the NMR work of Perrin and Gipe [11], who provided evidence that $NH_4{}^+$ can rotate fairly freely in water with a rate of the order of 10^{12} s^{-1}. This finding is surprising since ammonium ions are expected to form relatively strong and directional hydrogen bonds with water; facile bond breaking and reforming between NH_4^+ and H_2O does not conform to the commonly held picture of "hydrogen bonding." A disordered solvation environment presenting five H_2O molecules in the first shell has, thus, been suggested to account for the observed facile rotation. The suggestion of loose coupling of ammonium ions with surrounding water molecules is indeed supported by molecular dynamics calculations [10].

We have previously [12–14] successfully observed the spectra of $NH_4^+(NH_3)_n$ and $H_3O^+(H_2O)_n$ in a supersonic jet using vibrational predissociation spectroscopy (VPS). The success of these observations indicates that VPS is well suited to the investigation of NH_4^+ hydration in the gas phase. Such an investigation correlates well with studies on heterogeneous water nucleation [15] and cluster ion chemistry in the stratosphere [16]. As is generally known, heterogeneous nucleation occurs more frequently than homogeneous nucleation because charge-dipole Coulombic interactions have a greater tendency than van der Waals forces to attract molecules around the ion core to form clusters [17]. Presently, the number of spectroscopic investigations on the structure and bonding of cluster ions, such as $H_3O^+(H_2O)_n$, that are important in the atmosphere and in solution phases remains limited. Choi et al. [18] recently studied the intracluster reactions of $NO^+(H_2O)_n$ to rationalize the predominance of $H_3O^+(H_2O)_n$ in the D region of the ionosphere. Mikami and co-workers [19] investigated [phenol-$(H_2O)_n$]$^+$ clusters and found that proton transfer from $C_6H_5OH^+$ to H_2O occurs at $n = 3$. Weinheimer and Lisy [20] explored clustering of water around Cs^+ ions, $Cs^+(H_2O)_{1-5}$, and established the first infrared spectroscopic characterization of metal ion-water clusters in a molecular beam. The last work, concerning hydration of metallic ions, is fundamentally important in solution chemistry.

In this paper, we provide a critical overview of our investigation on the hydration mechanism of ammonium ions in a corona-discharged molecular beam using vibrational predissociation spectroscopy. We systematically monitored how the frequencies of the NH and OH stretching varied with the number of solvent molecules to investigate the influence of solvent molecules on the ion core vibrations. We also compared our observations with those of $H_3O^+(H_2O)_n$ and $CH_3NH_3^+(H_2O)_n$ in an effort to understand the nature of water nucleation on protonated ions. This comparison is expected to help elucidate how water molecules are interconnected through hydrogen bonding with each other and with the ion core, i.e. the mechanism of charge-induced cloud formation by protonated ions. The influence of ion core properties on cluster structures can, thereby, be examined.

2. Experimental

Details of the spectroscopic methods and the ion beam apparatus have been previously described [12,14,21]. Briefly, we synthesized the ammonium ions by corona discharging a flow of NH_3/H_2O vapor seeded in pure H_2. The ions were then supersonically expanded through a 75 μm nozzle to form complexes with H_2O. Since the proton affinity of NH_3 exceeds that of H_2O by 37.5 kcal mol^{-1} [1], NH_4^+ was preferentially formed [22].* The route to the synthesis of ammonium ion-water clusters in the supersonic beam is believed to proceed as follows:

$$H_2 + e^- \rightarrow H_2^+ + 2e^- \tag{2}$$

$$H_2^+ + H_2 \rightarrow H_3^+ + H \tag{3}$$

$$NH_3 + H_3^+ \rightarrow NH_4^+ + H_2 \tag{4}$$

$$H_2O + H_3^+ \rightarrow H_3O^+ + H_2 \tag{5}$$

$$NH_3 + H_3O^+ \rightarrow NH_4^+ + H_2O \tag{6}$$

$$NH_4{}^+ + H_2O + M \rightarrow NH_4^+(H_2O) + M^* \tag{7}$$

$$NH_4^+(H_2O)_{n-1} + H_2O + M \rightarrow NH_4^+(H_2O)_n + M^* \tag{8}$$

Owing to the corona discharge, the internal temperature of the clusters is relatively high, ~150 K [21]. To verify the presence of structural isomers, the beam temperature was varied by adjusting the source nozzle temperature from 310 to 250 K and the nozzle backing pressure from 50 to 200 Torr. The adjustments allowed a change in beam temperature of about ±20 K.

Spectra of the cluster ions were obtained using a vibrational predissociation ion trap (VPIT) spectrometer and a pulsed infrared laser system. The unique feature of this VPIT spectrometer lies in the fact that it is a tandem mass spectrometer with an octopole ion trap sitting between these two mass filters. A magnet sector, with a mass resolution exceeding 200, first selects the ions of interest [$NH_4^+(H_2O)_n$] to be stored in the ion trap for about 1 ms. The storage considerably reduces the number of metastable ions by internally cooling off the clusters via thermal evaporation. Vibrational predissociation† follows when the ion clusters are resonantly excited by infrared laser photons as

$$NH_4^+(H_2O)_n \rightarrow NH_4^+(H_2O)_{n-1} + H_2O \tag{9}$$

The daughter ions [$NH_4^+(H_2O)_{n-1}$] are then detected by a quadrupole mass spectrometer to obtain a background-minimized spectrum. As previously demonstrated [21] in an elaborate power dependence measurement, the vibrational predissociation involved herein is a one-photon excitation process. While the lower mass clusters have hydration energies higher than 10 kcal mol^{-1} per water molecule [8], one

---

* Ab initio calculations indicate that there is no barrier in this proton transfer process.

† Direct time measurements revealed that the photodissociation finishes in 20 μs.

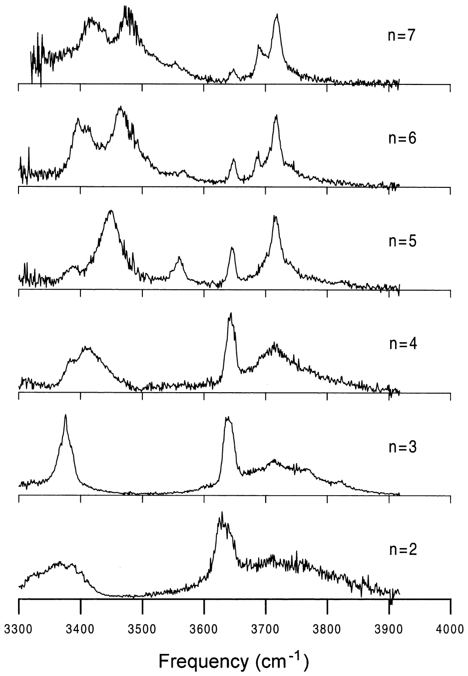

Fig. 1. Vibrational predissociation spectra of $NH_4^+(H_2O)_n$ in the OH stretching region. All the spectra are laser power normalized. The typical nozzle temperature and backing pressure used in obtaining these spectra were 300 K and 60 Torr, respectively.

infrared photon with an energy level of 8–11 kcal mole^{-1} at 2700–3900 cm^{-1} is sufficient to dissociate the clusters at the expense of excess internal energy.

3. Results and analysis

3.1. The OH stretches (3300–3900 cm^{-1})

Fig. 1 systematically compares the vibrational predissociation spectra of $NH_4^+(H_2O)_{2-7}$ in the OH stretching region. At $n = 2$ and 3, only one group of transitions was observed at 3600–3900 cm^{-1}. The frequencies of these transitions are close to those of free H_2O at 3657 and 3756 cm^{-1} [23], and they can be assigned to the stretching motions of two coupled O–H bonds whose H atoms do not participate in hydrogen bonding. The H_2O molecules in these two protonated clusters act as a proton acceptor upon hydrogen bond formation. The sharper transitions at 3636 ± 4 cm^{-1} are due to symmetric free OH stretches, and the more complex features peaking at 3719 ± 1 cm^{-1} are due to the K rotationally coupled asymmetric stretching of the neutral H_2O molecules. The congestion in the K rovibrational lines of the latter is a combined result of rapid vibrational predissociation, small rotational constants of the clusters, dipole–dipole coupling between neighboring H_2O molecules, and a relatively high rotational temperature owing to the corona discharge. The molecular structures corresponding to the observed spectra are illustrated in Fig. 2(a) and (b).

For $NH_4^+(H_2O)_4$, an additional feature emerges at 3408 cm^{-1}, and it can be ascribed to hydrogen bonded OH stretches. Compared with that of free OH stretching, it is lower in frequency because hydrogen bonding tends to weaken the valence OH bond of the donor, resulting in a larger red shift. This OH absorption appears abruptly at $n = 4$, suggesting that the fourth H_2O can be hydrogen bonded to one of the three H_2O molecules comprising the first solvation shell. Importantly, the observation reveals, for the first time, the presence of structural isomers at n as small as 4 in the free jet expansion. The structural isomerization can be even better observed at $n = 5$, where three well-separated bands at 3383, 3449, and 3559 cm^{-1} arise from three different isomers [21,24]. Accompanying the changes of $n = 4 \rightarrow 5$ is the emergence of the sharp feature centering at 3717 cm^{-1}, which is the free OH stretching of H_2O in the form of double hydrogen bonding, or the two-coordinated H_2O.

The bonded OH stretching absorptions intensify as the solvation number increases to $n = 6$. Additionally, they are broadened and spread widely in frequency from 3300–3600 cm^{-1} at $n = 7$. The broadening and congestion are believed to be the result of band overlapping of many possible hydrogen bonded OH stretches and also the presence of many possible low-energy isomers. Contrary to the hydrogen bonded OH stretches, the free OH stretching absorptions of two-coordinated H_2O remain narrow. For $NH_4^+(H_2O)_6$, an additional sharp absorption emerges at 3688 cm^{-1}, which becomes more prominent at $n = 7$. The intensity increase of this feature is opposite to the diminishing of the symmetric free OH

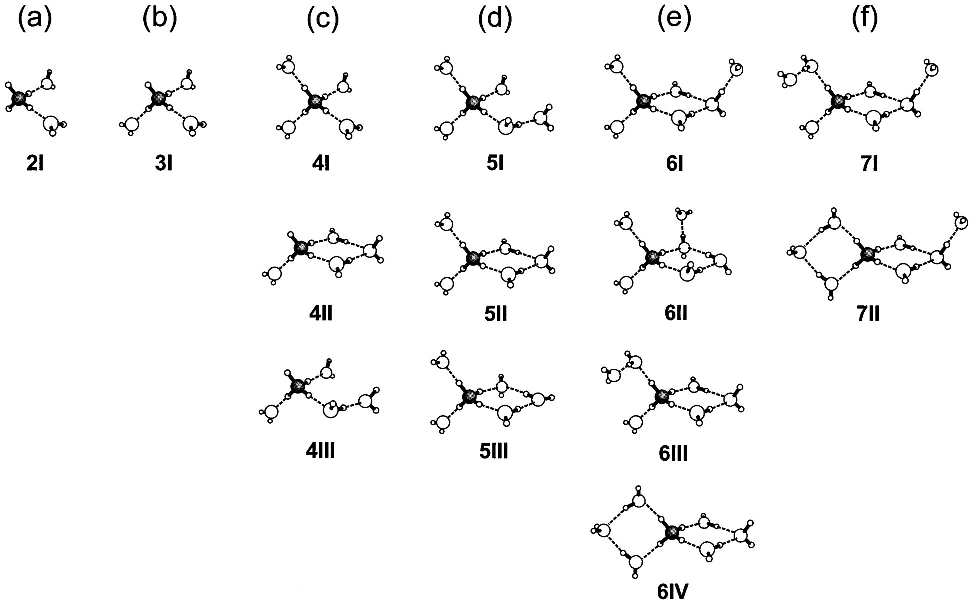

Fig. 2. Ab initio optimized geometries of $NH_4^+(H_2O)_{2\text{–}7}$. The order of calculated stability using B3LYP/6-31+G* for $NH_4^+(H_2O)_{4-6}$ isomers is 4I > 4II > 4III, 5II > 5I > 5III, and 6I > 6IV > 6III > 6II (see [21] and [26] for details). The N,O,H atoms are denoted by filled, large open, and small open circles, respectively.

stretching absorption at 3634 cm^{-1} discussed earlier. Since the 3688 cm^{-1} band has been previously assigned to the free OH stretching of three-coordinated H_2O [24], this contrast suggests that, in $NH_4{}^+(H_2O)_7$, most of the hydrogen atoms of the water molecules are no longer free but are heavily involved in hydrogen bonding.

3.2. The NH stretches (2700–3400 cm^{-1})

Fig. 3 summarizes the vibrational predissociation spectra of $NH_4^+(H_2O)_{2\text{–}7}$ in the hydrogen bonded NH stretching region from 2600–3300 cm^{-1}. They can be compared with the nonhydrogen bonded NH stretches at 3300–3400 cm^{-1}, as depicted in Fig. 1. The figure clearly illustrates the evolution of spectral complexity as n increases. At $n = 2$, the cluster exhibits symmetric and asymmetric stretching absorptions at 2831 and 2961 cm^{-1}, respectively, for bonded NH. These features are intense but broad, characteristic of hydrogen bonded stretches. For the free NH stretching, coupling of the two NH oscillators gives rise to a broadband peaking at 3363 cm^{-1}. Deconvolution of the feature with two Gaussian profiles suggests band origins of 3326 and 3378 cm^{-1} with a full width at half maximum (FWHM) of 60 cm^{-1} for each absorption. The results correspond well to the structure 2I displayed in Fig. 2(a) where the four NH bonds form two pairs of free and hydrogen bonded oscillators. The assignment of these stretches is corroborated by the observation of the $NH_4^+(H_2O)_3$ spectra, where a single, sharp free NH stretching absorption is found at 3375 cm^{-1}. For $NH_4^+(H_2O)_3$, two distinct features are observed at 2962 and 3045 cm^{-1} in Fig. 3, and they can be assigned to the symmetric and asymmetric stretching of the three bonded NH oscillators, respectively. The structures hereby revealed are in good accord with that deduced from the OH stretching spectra shown in Fig. 1.

Upon adding the fourth H_2O to NH_4^+, the spectrum is not simplified as originally expected for $NH_4^+(H_2O)_4$ with a completed first solvation shell. Temperature dependence measurements and ab initio calculations indicate that the most prominent feature peaking at 3116 cm^{-1} should be the asymmetric NH stretching absorption of the completely solvated NH_4^+

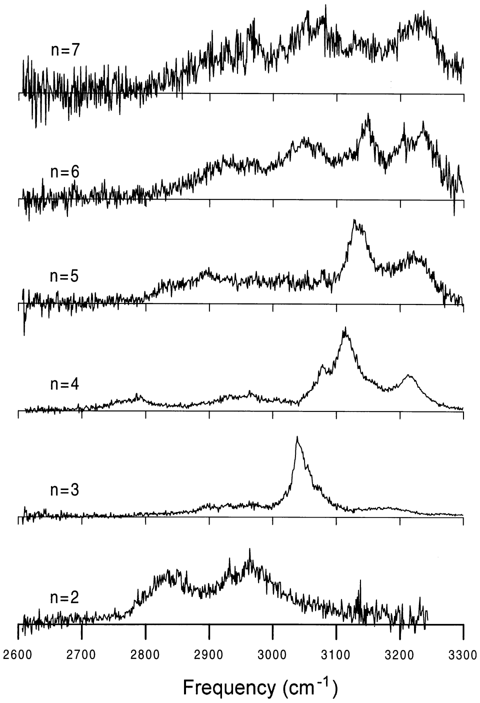

Fig. 3. Vibrational predissociation spectra of $NH_4^+(H_2O)_n$ in the NH stretching region. All the spectra are laser power normalized. The typical nozzle temperature and backing pressure used in obtaining these spectra were 300 K and 60 Torr, respectively.

ion core [21], as isomer 4I illustrated in Fig. 2(c). The higher frequency feature at 3213 cm^{-1} is likely due to H_2O bending overtones or the combination mode of the valence NH stretching with hydrogen bond vibrations of ~100 cm^{-1}. The additional features appearing on the lower frequency side are the absorptions of other isomers. This observation of isomers agrees closely with the earlier conclusion reached based on the OH stretching spectra that structural isomerization is energetically allowed upon completion of the first hydration shell. At $n \geq 5$, the hydrogen bonded NH stretching spectra become rather complicated and practically unassignable. However, it is noticed by comparing the spectra of $n = 4$ and 5 that further addition of H_2O to $NH_4^+(H_2O)_4$ does not drastically change the spectra of the ion core stretches.

We note that while some complexities exist in the spectra of Fig. 3, the predominant features evolve regularly from 2900–3100 cm^{-1} at $n = 2$–5. For the nonhydrogen bonded NH, the stretching absorptions situate fairly constantly at 3375 ± 15 cm^{-1} for $NH_4{}^+(H_2O)_{2-4}$. At $n = 4$, the absorption is considerably overlapped by that of the hydrogen bonded OH stretches resonant nearly at the same frequency; fortunately, they can be separated following careful spectral deconvolution. For the hydrogen bonded NH stretches, the vibrations resonate at 2831 and 2961 cm^{-1} at $n = 2$. On average, they red shift 447 cm^{-1} from the asymmetric stretching of NH_4^+ [25] isolated in the gas phase. The magnitude of the red shifting decreases markedly with n and gradually levels off at $n = 5$. This decrease in red shifting correlates qualitatively well with the weakening of the hydrogen bonds with an increasing n (Table 1).

4. Discussion

4.1. Identification of isomeric structures and ring opening–closing dynamics

The identification of structural isomers at $n \geq 4$ was accomplished by systematic temperature dependence measurements and ab initio calculations [21]. Fig. 4 illustrates the vibrational predissociation spectrum of $NH_4^+(H_2O)_4$, in which the relative absorption intensities of the bands at 3408 and 3543 cm^{-1} are seen to vary independently with the beam temperature. Earlier calculations [7] predicted that the ammonium ion completes its first hydration shell at $n = 4$ with all four H atoms taken by the surrounding H_2O. This symmetric structure is ~2 kcal mol^{-1} more stable than the asymmetric isomer 4III depicted in Fig. 2(c). Interestingly, the asymmetric isomer can indeed be observed in this experiment for its characteristic bonded OH stretching absorption at 3408 cm^{-1} [21]. Also, the gradual disappearance of this isomer at a lower beam temperature is in good agreement with the energetics predictions [7]. The third form of the cluster that can be identified presently, but was not predicted previously, is the ring shaped isomer 4II. The isomer displays a characteristic bonded OH stretching absorption at 3543 cm^{-1} and appears only when the beam is sufficiently cold,

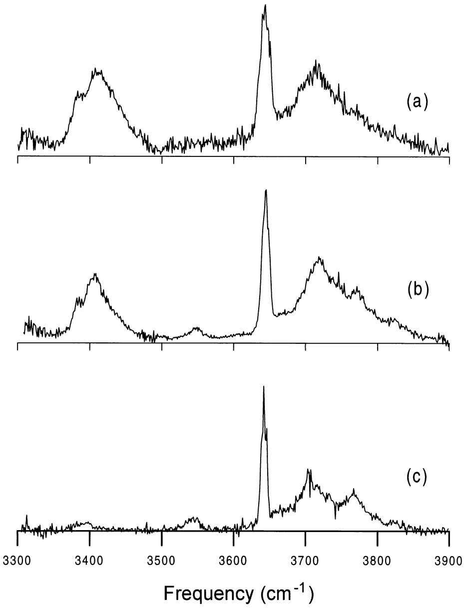

Fig. 4. Temperature dependence of the vibrational predissociation spectrum of $NH_4^+(H_2O)_4$. The spectra were obtained at a nozzle temperature and a backing pressure of (a) (300 K, 60 Torr), (b) (260 K, 60 Torr), and (c) (270 K, 130 Torr), respectively. The independent change of the band intensities at 3408 and 3543 cm^{-1} reveals the presence of structural isomers.

indicating that it is substantially more stable than isomer 4III. The observations are consistent with the recent ab initio calculations of Jiang et al. [26], who found a difference of >0.5 kcal mol^{-1} in stability between these two isomeric forms.

Fig. 2(d) presents three optimized geometries of $NH_4^+(H_2O)_5$ obtained by means of ab initio calculations [21,26]. The symmetric ring structure denoted by 5II is predicted to be most stable for about 2 kcal mol^{-1} among the three isomers. Our temperature dependence measurements in Fig. 5 revealed their existence in the bonded OH stretches at 3562 and 3449 for isomers 5II and 5I, respectively. Remarkably, the spectrum displays a dramatic temperature dependence with the ring isomer essentially dominating the population as the beam temperature is lowered. It amounts to roughly 70% of the total isomers in population at the lowest beam temperature [Fig. 5(d)] that we could achieve in this experiment. Estimation of the beam temperatures by measuring the rate of metastable ion decomposition indicated that the internal temperature decreased from 160 to 130 K when the spectra in Fig. 5(a)–(d) were obtained [21].

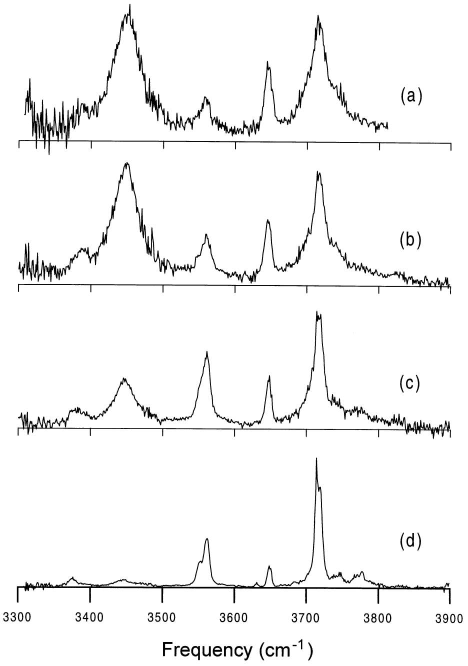

Fig. 5. Temperature dependence of the vibrational predissociation spectrum of $NH_4^+(H_2O)_5$. The spectra were obtained at a nozzle temperature and a backing pressure of (a) (360 K, 110 Torr), (b) (300 K, 60 Torr), (c) (280 K, 80 Torr), and (d) (250 K, 200 Torr), respectively. The independent change of the band intensities at 3376, 3449, and 3562 cm^{-1} reveals the presence of structural isomers.

Depicted in Fig. 2(e) are four low-energy isomers of $NH_4^+(H_2O)_6$. Isomer 6I is expected to be the predominant species since it is >0.5 kcal mol^{-1} [21] more stable than the other three isomeric forms and, furthermore, it can be synthesized more easily from 5I and 5II. Uniquely, this isomer contains a three-coordinated water molecule in addition to two-coordinated ones. The free OH stretching of the three-coordinated H_2O resonates at 3688 cm^{-1}, compared to 3719 cm^{-1} of the two-coordinated. The former exhibits a larger frequency red-shift since this water molecule experiences a larger perturbation from its nearest neighbors due to triple hydrogen bond formation. The other two isomers, 6III and 6IV, may also be present in the beam since the characteristic absorptions of the bonded OH stretches involved in the four-membered ring can also be observed in Fig. 1 at ~3550 cm^{-1} [21]. Notably, the intriguing double-ring isomer (6IV) is lower in energy than its ring opened partner (6III) by ~0.7 kcal mol^{-1} and, thus, it can be synthesized more easily in the jet.

The present investigation provides first spectroscopic evidence for the structural evolution of $NH_4^+(H_2O)_n$ from a single ring at $n = 4$ to a double ring at $n = 6$ [21]. This unique double-ring structure, with a symmetry of D_{2d}, is inherited naturally from the tetrahedral geometry of the ammonium central ion. For the cluster ion $NH_4^+(H_2O)_7$, however, assignments of the spectral features become considerably more difficult because the number of stable isomers increases exponentially with n. Fig. 2(f) displays two low-energy structures that contain a four-membered ring and a three-coordinated H_2O. It is highly likely that these two species are synthesized in this experiment since the free OH stretching of the three-coordinated H_2O can be clearly observed in Fig. 1 at 3691 cm^{-1}. The observation of this band is indicative of cubic construction in water networks.

The temperature dependence measurements of $NH_4^+(H_2O)_{4,5}$ in Figs. 4 and 5 reveal an intriguing ring opening and closing process. One can either close the symmetrically shaped ring by producing the clusters at a lower beam temperature or, conversely, leave the ring open in the beam with a higher temperature. This suggests an active means of studying hydrogen bond rearrangement dynamics in water-containing clusters [27]. Among these clusters, $NH_4^+(H_2O)_5$ presents itself as a model system for this study, since isomers 5I and 5II display two distinct absorptions in their bonded OH stretches. The unique feature allows the isomeric transition via hydrogen bond breaking and reforming between them to be closely examined. Starting with 5II, we have attempted to intentionally open the ring by colliding the cluster with H_2 at a pressure of 2×10^{-5} Torr in the octopole ion trap region. The ring was successfully opened, as evidenced by the increase in the relative absorption intensity of 5I versus 5II. The preliminary results for this intriguing ring opening and closing dynamics are presented in Fig. 6. The study along this direction is expected to provide fundamental insight into the intricate processes occurring in aqueous solutions [28].

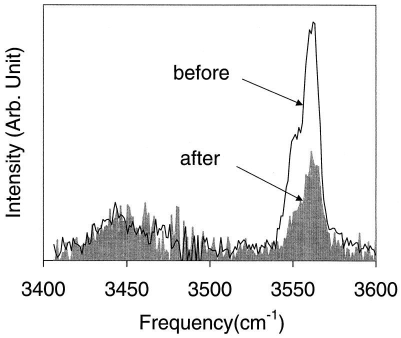

Fig. 6. Spectral changes induced by colliding H_2 with $NH_4^+(H_2O)_5$ at a pressure of $P_{H_2} = 2 \times 10^{-5}$ Torr in the octopole ion trap region. Comparing the $NH_4{}^+(H_2O)_5$ spectra obtained before and after the collision reveals a change in the relative intensity of the two features at 3449 and 3562 cm^{-1}. The relative intensity increase at 3449 cm^{-1}, which is due to the absorption of the ring-opened isomer 5I, is indicative of an isomeric transition of 5II → 5I, i.e. a ring opening process.

4.2. Comparison with $NH_4^+(NH_3)_n$, $CH_3NH_3^+(H_2O)_n$ and $H_3O^+(H_2O)_n$

We note from Fig. 3 that in the absence of structural isomers 4II and 4III, the $NH_4^+(H_2O)_4$ spectrum should exhibit only a single feature centering at 3116 cm^{-1} in the NH stretching region. This feature arises from the asymmetric stretching of the ion core shelled by one layer of water molecules. Relative to $\nu_3 = 3343$ cm^{-1} of free $NH_4{}^+$ [25], the stretching frequency of the hydrated ion is lower by 227 cm^{-1}. The magnitude of the red-shifting is considerably smaller than that of its analog $NH_4^+(NH_3)_4$ where a corresponding band origin at 2880 cm^{-1} was determined [14]. This result, however, is not unexpected because it has been previously illustrated in the study of NH_4^+-Ar_n [29] that the red shift directly reflects the strength of bonding between two individual constituents. A comparison of the hydrogen bond strengths and the ion core stretching frequencies between $NH_4^+(H_2O)_n$ and $NH_4^+(NH_3)_n$ at $n = 2$–7 is given in Tables 1 and 2, respectively.

We may associate $NH_4^+(H_2O)_n$ with its amine analog, $CH_3NH_3^+(H_2O)_n$. The spectra of these two

Table 2
Comparison of some characteristic frequencies of the ion core NH stretches between $NH_4^+(H_2O)_n$ and $NH_4^+(NH_3)_n$

	Frequencies (cm^{-1})		
n	$NH_4^+(H_2O)_n$[a]	$NH_4^+(NH_3)_n$[b]	Assignments
2	3363	3392, 3395	NH_4^+ free NH sym. & asym. str.
	2831, 2961		NH_4^+ bonded NH sym. & asym. str.
3	3375	3365	NH_4^+ free NH str.
	2962, 3045	2660, 2692	NH_4^+ bonded NH sym. & asym. str.
4	3382, 3391		NH_4^+ free NH str.
	2779, 2959, 3075, 3116	2865	NH_4^+ bonded NH str.
5	2892, 3080, 3133	2650, 2880, 2910	NH_4^+ bonded NH str.
6	2960, 3053, 3146	2720, 2910, 2950	NH_4^+ bonded NH str.
7	2951, 3070, 3139	2770, 2955	NH_4^+ bonded NH str.

[a] See [21] for detailed assignments.
[b] [14].

species share many similarities in the OH stretching region but differ considerably in the ion core vibrations. At 2600–3300 cm^{-1}, the spectra of $CH_3NH_3^+(H_2O)_n$ are blended with the absorptions of NH and CH stretching in near resonance. They are also complicated by the presence of structural isomers, water bending overtones, and ion core combination bands [21]. Unambiguous assignment of the spectral features is, thus, hampered by these complexities and also by the lack of the vibrational spectrum of free $CH_3NH_3^+$ for comparison. Fig. 7(b) displays a typical OH stretching spectrum of the hydrated methylammonium ion $CH_3NH_3^+(H_2O)_4$. Systematic investigation of $CH_3NH_3^+(H_2O)_{2-6}$ indicates that the four-membered ring isomer forms at $n = 4$, yielding a characteristic absorption at 3550 cm^{-1}. The frequency agrees with that of $NH_4^+(H_2O)_5$ to within 10 cm^{-1}. The emergence of this feature at $n = 4$ correlates well with $n = 5$ of $NH_4^+(H_2O)_n$ because one of the NH sites is taken by the methyl group in $CH_3NH_3^+(H_2O)_n$. Also in line with $NH_4^+(H_2O)_6$, the $CH_3NH_3^+(H_2O)_5$ displays a free OH stretching absorption of three-coordinated H_2O at 3686 cm^{-1} [24]. The structures suggested by the VPS of $CH_3NH_3^+(H_2O)_{4,5}$ are depicted in Fig. 8(a).

Spectral comparison can also be made with $H_3O^+(H_2O)_4$. The hydronium ion has one pair of free electrons that do not participate in hydrogen bonding; hence, one would expect a four-membered ring to be formed at $n = 4$ as in $CH_3NH_3^+(H_2O)_n$. This expectation, however, is at variance with our observation in Fig. 7 where clear evidence of the four-membered ring formation can be found for both $NH_4^+(H_2O)_5$ and $CH_3NH_3^+(H_2O)_4$ at ~3550 cm^{-1}, but is absent for

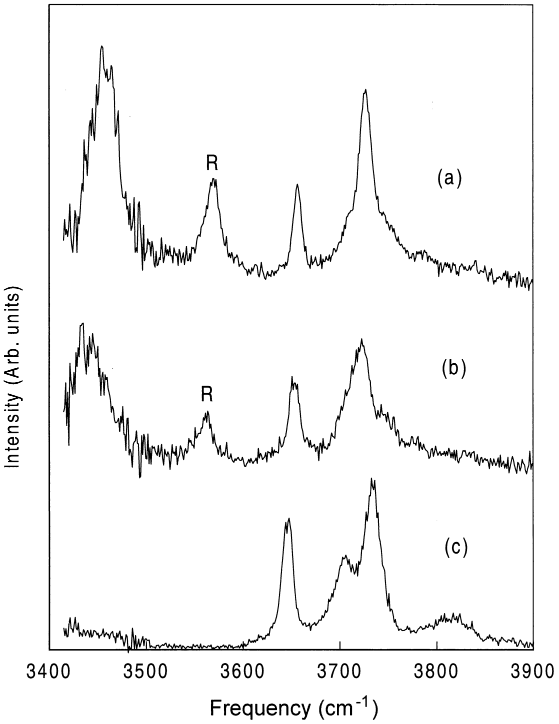

Fig. 7. Vibrational predissociation spectra of (a) $NH_4^+(H_2O)_5$, (b) $CH_3NH_3^+(H_2O)_4$, and (c) $H_3O^+(H_2O)_4$ in the OH stretching region. The features denoted by R are the characteristic hydrogen bonded OH stretching absorptions of four-membered ring vibrations.

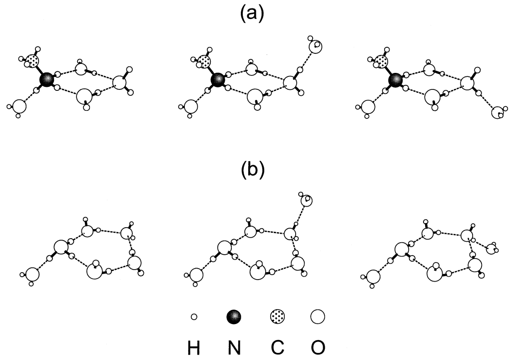

Fig. 8. The experimentally observed and ab initio predicted geometries of (a) $CH_3NH_3^+(H_2O)_{4,5}$ and (b) $H_3O^+(H_2O)_{5,6}$.

$H_3O^+(H_2O)_4$. Although ab initio calculations [30] predict that a four-membered ring would be one of the low-energy structures of $H_3O^+(H_2O)_4$, this ring formation appears to be kinetically unfavored in the free jet expansion. As will be presented elsewhere [30], the hydronium ion clearly forms a five-membered ring with water, which is evidenced by the bonded OH stretching absorption at 3517 cm^{-1} for $H_3O^+(H_2O)_5$ and the free OH stretching of three-coordinated H_2O at 3682 cm^{-1} for $H_3O^+(H_2O)_6$ [13]. The observation of the 3682 cm^{-1} band reveals a three-dimensional arrangement where the fifth H_2O molecule can be situated either at the top of or underneath the ring plane. The five-membered ring and its associated structures are illustrated in Fig. 8(b). (The preference of five-membered ring formation can be attributed to the large angle (115°) held by the two interconnected O–H bonds of H_3O^+ [25]. This may be compared to the corresponding angle of 109° for NH_4^+ and 107° for $CH_3NH_3^+$ [26].)

The hydrophobic nature of the methyl group in $CH_3NH_3^+(H_2O)_n$ leads to clustering of water molecules on the other side of the ion core. For $H_3O^+(H_2O)_n$, ab initio calculations [30] indicate that H_2O prefers to act as a proton acceptor rather than as a donor; therefore, the electron lone pair of the ion core is free of hydrogen bonding upon hydration. In the present experiment, we found no evidence that water molecules are bonded to the methyl group of $CH_3NH_3^+(H_2O)_n$ or to the lone pair electrons of $H_3O^+(H_2O)_n$ at the solvation number up to $n = 8$ [13,30]. It would be of interest to explore when these processes start to occur. A question related to this subject has been previously addressed by ab initio calculations which consider the potential anisotropy of the interaction between Ar and HF [31]. In Ar_nHF clusters, Ar preferentially attaches to the H end, making a cap on the top of the hydrogen atom at $n \leq 6$. The first solvation shell closes at $n = 12$ where an icosahedral cage composed of 18 triangular planes is formed. For $H_3O^+(H_2O)_n$ and $CH_3NH_3^+(H_2O)_n$, owing to strong hydrogen bonding between water molecules which tend to cluster together, the central ions are expected to be completely hydrated at a much larger n.

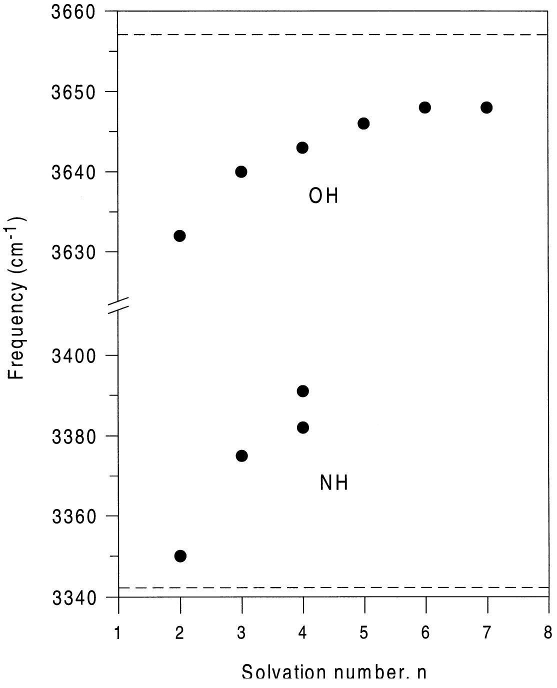

Fig. 9. Shifts of NH and OH stretching frequencies with n in $NH_4^+(H_2O)_n$ for the symmetric free OH stretches of H_2O in the form of a single proton acceptor and the free NH stretches of NH_4^+. Dashed lines denote separately the symmetric OH stretching frequency of free H_2O at 3657 cm^{-1} and the asymmetric NH stretching frequency of free NH_4^+ at 3343 cm^{-1}. The two data points of the NH stretches at $n = 4$ are due to two structural isomers.

4.3. Shift of stretching frequencies and approach to condensed phases

Our experiments on the three cluster ions demonstrated that structures of the ion cores strongly influence how the solvent network is constructed at a small n. In hydrated cations, such as $M^{m+}(H_2O)_n$ where $M^{m+} = Na^+$, Mg^{2+} and Al^{3+}, a coordination number of six for the first hydration shell has been predicted by ab initio calculations [32]. For $Cs^+(H_2O)_n$, a red-shift of ~15 cm^{-1} [20] was determined for the free OH stretching of such bonded H_2O, as compared to free H_2O. This shift is comparable to the corresponding red-shifts in the protonated ion-water complexes studied herein. Fig. 9 shows the frequency shifting of the symmetric free OH stretching of the singly hydrogen bonded H_2O at $n = 2$–7 in $NH_4^+(H_2O)_n$. The magnitude of the red-shift is reduced when the water molecules are situated further away from the ion center. Notably, the frequencies gradually converge at 3648 cm^{-1}, which is about 9 cm^{-1} lower than the corresponding resonance of free H_2O. This 9 cm^{-1} difference originates from the perturbation involving single hydrogen bond formation at the O end between water molecules at ~150 K.

The free OH stretching of two- and three-coordinated H_2O in protonated cluster ions correlates with the dangling OH stretches on crystalline ice [33] and liquid water surfaces [34]. On these surfaces, water molecules are predominantly three-coordinated. Infrared spectroscopy indicates that these three-coordinated dangling OH groups can display frequencies varying from 3720 cm^{-1} on amorphous ice to 3696 cm^{-1} on crystalline ice surfaces [33,35,36]. They may be compared to 3690 cm^{-1} in the present observations. We have recently accounted computationally for the wide frequency spread (3696–3720 cm^{-1}) by employing ab initio calculations for a number of benchmark clusters [37]. Systematic investigations of these clusters, such as water octamers, allow us to conclude that the variation of ~25 cm^{-1} is due to the disparity in molecular structures between different ice phases. We attribute the smaller frequency red-shift in amorphous ice, primarily, to the reduced directionality of the interconnected hydrogen bonds, $\angle O\text{–}H\cdots O < 180°$. For $NH_4^+(H_2O)_n$, while all the hydrogen bonds involved in the four-membered ring are slightly tilted with $\angle N\text{–}H\cdots O \sim \angle O\text{–}H\cdots O \sim 160°$, the frequency of the three-coordinated H_2O remains at ~3690 cm^{-1} [37]. The frequency, being ~25 cm^{-1} red-shifted from that of neutral water clusters, is a result of charge delocalization effects.

Also apparent in Fig. 1 is that as the cluster size increases to $n = 7$, the bonded OH stretches display a broad absorption centering at ~3450 cm^{-1}, on top of which narrower features can be found. Interestingly, the overall shape of the band profile resembles those of medium-sized water clusters [38,39] and liquid water, but is dissimilar to that of crystalline ice [40]. One can also properly account for these spectral similarities and dissimilarities by considering the structures of these phases. Since the higher degree of bond directionality results in stronger hydrogen bonding, as in crystalline ice, a larger frequency red-shift for the bonded OH stretches [41] is expected.* This effect is indeed observed for crystalline ice which displays a relatively sharp (FWHM ~200 cm^{-1}) absorption centering at ~3200 cm^{-1}. In liquid water and medium-sized water clusters, the bonded OH stretching frequencies span a wide range from 3000–3500 cm^{-1}. The absorptions at the high frequency side can be attributed to the bonded OH stretching of water molecules in the form of double proton donors [42]. These double proton donors are abundant in water-containing clusters but are absent in crystalline ice.

In addition to the OH stretches, the NH band origins also exhibit smooth blue-shifting as n increases. These shifts have important implications for understanding ammonium ion hydration in condensed phases, a subject which awaits further exploration by means of either infrared or Raman spectroscopy. Fig. 9 displays the shift in the free NH stretching frequency with n. The converging behavior of the shifting at a larger n is similar to that observed [12,14] and predicted [32] for a variety of cluster ions. The up-shifting in the NH stretching frequencies of the clusters from that of free NH_4^+ can be understood as being a result of charge delocalization of the central ion upon solvation. The delocalization effect increases with n and reaches a pleatau in the limit of

---

* The difference in bonded OH stretching frequencies is evident in the ab initio calculations of water octamer cubes and a trilobate water octamer that is one fragment of hexagonal ice lattice.

large clusters or, ultimately, aqueous solutions. Detailed comparisons of the observations with the calculations have been reported elsewhere [21,26].

5. Conclusion

The vibrational predissociation spectra of $NH_4^+(H_2O)_n$ cluster ions reveal a number of intriguing structural isomers synthesized by a free jet expansion. These clusters are the simplest hydrated amines explored and they have been examined in detail by studying their characteristic NH and OH stretching vibrations. Notably, the system can be regarded as a prototype for investigating how amino groups interact with water molecules upon hydrogen bond formation in solution phases. It is hoped that the present studies will help elucidate the mechanism of complex hydrogen bonding and hydrophobic interactions existing in many biologically important systems whose investigations have attracted increasing attention in recent years.

Acknowledgements

We thank the Academia Sinica and the National Science Council (Contract No. NSC 87-2113-M-001-036) of Taiwan, Republic of China, for financial support.

References

[1] S.G. Lias, J.F. Liebman, R.D. Levin, J. Phys. Chem. Ref. Data 13 (1984) 695.
[2] S.S. Wee, S. Kim, M.S. Jhon, H.A. Scheraga, J. Phys. Chem. 94 (1990) 1656.
[3] S. Okouchi, T. Moto, Y. Ishihara, H. Numajiri, H. Uedaira, J. Chem. Soc. Faraday Trans. 92 (1996) 1853.
[4] P. Kebarle, Annu. Rev. Phys. Chem. 28 (1977) 455.
[5] E.J. Bieske, J.P. Maier, Chem. Rev. 93 (1993) 2603.
[6] J.C. Contador, M.A. Aguilar, F.J. Olivares del Valle, Chem. Phys. 214 (1997) 113, and references therein.
[7] E. Kassab, E.M. Evleth, Z.D. Hamou-Tahra, J. Am. Chem. Soc. 112 (1990) 103.
[8] M. Meot-Ner, J. Am. Chem. Soc. 106 (1984) 1265.
[9] W.L. Jorgensen, J. Gao, J. Phys. Chem. 90 (1986) 2174.
[10] O.A. Karim, A.D.J. Haymet, J. Chem. Phys. 93 (1990) 5961.
[11] C.L. Perrin, R.K. Gipe, Science 238 (1987) 1393.
[12] L.I. Yeh, M. Okumura, J.D. Myers, J.M. Price, Y.T. Lee, J. Chem. Phys. 91 (1989) 7319.
[13] M.W. Crofton, J.M. Price, and Y.T. Lee, in Clusters of Atoms and Molecules, H. Haberland (Ed.), Springer Verlag, Berlin, 1994, Vol. II, p. 44.
[14] J.M. Price, M.W. Crofton, Y.T. Lee, J. Phys. Chem. 95 (1991) 2182.
[15] J.L. Katz, J.A. Fisk, V.M. Chakarov, J. Chem. Phys. 101 (1994) 2309.
[16] E.E. Ferguson, F. Arnold, Acc. Chem. Res. 14 (1981) 327.
[17] R.P. Wayne, Chemistry of Atmospheres, Oxford University Press, Oxford, 1991.
[18] J.-H. Choi, K.T. Kuwata, B.-M. Haas, Y. Cao, M.S. Johnson, M. Okumura, J. Chem. Phys. 100 (1994) 7153.
[19] T. Ebata, A. Fujii, N. Mikami, Int. J. Mass Spec. Ion Processes 159 (1996) 111.
[20] C.J. Weinheimer, J.M. Lisy, J. Chem. Phys. 105 (1996) 2938.
[21] Y.-S. Wang, H.-C. Chang, J.C. Jiang, S.H. Lin, Y.T. Lee, H.-C. Chang, J. Am. Chem. Soc. (unpublished).
[22] H.-H. Bueker, E. Uggerud, J. Phys. Chem. 99 (1995) 5945.
[23] G. Herzberg, Molecular Spectra and Molecular Structure, III. Electronic Spectra and Electronic Structure of Polyatomic Molecules, Van Nostrand-Reinhold, New York, 1966.
[24] Y.-S. Wang, J.C. Jiang, C.-L. Cheng, S.H. Lin, Y.T. Lee, H.-C. Chang, J. Chem. Phys. 107 (1997) 9695.
[25] C.S. Gudeman, R.J. Saykally, Ann. Rev. Phys. Chem. 35 (1984) 387.
[26] J.C. Jiang, H.-C. Chang, Y.T. Lee, S.H. Lin (unpublished).
[27] D.J. Wales, I. Ohmine, J. Chem. Phys. 98 (1993) 7257.
[28] A. Luzar, Faraday Discuss. 103 (1996) 29.
[29] O. Dopfer, S.A. Nizkorodov, M. Meuwly, E.J. Bieske, J.P. Maier, Int. J. Mass Spectrom. Ion Processes 167/168 (1997) 637.
[30] J.C. Jiang, H.-C. Chang, S.H. Lin, Y.T. Lee, H.-C. Chang (unpublished).
[31] S. Liu, Z. Bacic, J.W. Moskowitz, K.E. Schmidt, J. Chem. Phys. 100 (1994) 7166.
[32] M.M. Probst, K. Hermansson, J. Chem. Phys. 96 (1992) 8995.
[33] B. Rowland, N.S. Kadagathur, J.P. Devlin, V. Buch, T. Feldman, M.J. Wojcik, J. Chem. Phys. 102 (1995) 8328, and references therein.
[34] Q. Du, R. Superfine, E. Freysz, Y.R. Shen, Phys. Rev. Lett. 70 (1993) 2313.
[35] A. Givan, A. Loewenschuss, C.J. Nielsen, J. Phys. Chem. B 101 (1997) 8696.
[36] M.A. Zondlo, T.B. Onsasch, M.S. Warshawsky, M.A. Tolbert, G. Mallick, P. Arentz, M.S. Robinson, J. Phys. Chem. B 101 (1997) 10887.
[37] J.C. Jiang, J.-C. Chang, B.-C. Wang, S.H. Lin, Y.T. Lee, H.-C. Chang, Chem. Phys. Lett. 289 (1998) 373.
[38] D.F. Coker, R.E. Miller, R.O. Watts, J. Chem. Phys. 82 (1985) 3554.
[39] R.H. Page, M.F. Vernon, Y.R. Shen, Y.T. Lee, Chem. Phys. Lett. 141 (1987) 1.
[40] J.E. Bertie, E. Whalley, J. Chem. Phys. 40 (1964) 1637.
[41] D.A. Estrin, L. Paglieri, G. Corongiu, E. Clementi, J. Phys. Chem. 100 (1996) 8701.
[42] R.N. Pribble, T.S. Zwier, Science 265 (1994) 75.